



**HAL**  
open science

## Multi-objective optimization of the sizing of a hybrid electrical vehicle

Vincent Reinbold, Laurent Gerbaud, Emmanuel Vinot

► **To cite this version:**

Vincent Reinbold, Laurent Gerbaud, Emmanuel Vinot. Multi-objective optimization of the sizing of a hybrid electrical vehicle. *International Journal of Applied Electromagnetics and Mechanics*, 2017, Selected papers from the 13th International Workshop on Optimization and Inverse Problems in Electromagnetism (OIPE 2014), 53 (S2), pp.S179-S190. 10.3233/JAE-140160 . hal-01488045

**HAL Id: hal-01488045**

**<https://hal.science/hal-01488045v1>**

Submitted on 13 Mar 2017

**HAL** is a multi-disciplinary open access archive for the deposit and dissemination of scientific research documents, whether they are published or not. The documents may come from teaching and research institutions in France or abroad, or from public or private research centers.

L'archive ouverte pluridisciplinaire **HAL**, est destinée au dépôt et à la diffusion de documents scientifiques de niveau recherche, publiés ou non, émanant des établissements d'enseignement et de recherche français ou étrangers, des laboratoires publics ou privés.

# MULTI-OBJECTIVE OPTIMIZATION OF THE SIZING OF A HYBRID ELECTRICAL VEHICLE

Vincent REINBOLD\*\*\*, Laurent GERBAUD\* and Emmanuel VINOT\*\*

\* Univ. Grenoble Alpes, G2eLab (CNRS UMR5269, INPG, UJF), F-38142 Cedex, Grenoble, France  
vincent.reinbold@g2elab.grenoble-inp.fr

\*\* IFSTTAR, LTE, 25 av. François Mitterrand, 69675, Bron, France  
emmanuel.vinot@ifsttar.fr

**Abstract.** Hybrid electrical vehicles involve two sources of energy, usually gasoline and electricity. The energy management determines the power sharing between the internal combustion engine and the electrical machine (EM). It is highly dependent on the driving cycle (i.e. the use of the vehicle). In this context, the optimal sizing of the EM is determined by: the driving cycle, the power-train characteristics (i.e. ratios and physical limitations e.g. maximum torque available) and the energy management. The key idea of this work is to involve the driving cycle and the environment of the electrical machine in a global multi-objective optimization process taking into account an optimal energy management and an accurate model of the EM based on magnetic circuit equivalent model.

**Keywords:** Electrical machine, hybrid electrical vehicle, magnetic equivalent circuit, sizing, energy management, multi-objectives optimization.

## 1. Introduction

Hybrid electrical vehicles (HEV) represent an innovative solution to reduce pollutant emission and fuel consumption. A possible configuration of the HEV is a parallel two-clutch architecture (Fig. 1). In this architecture, both Internal Combustion Engine (ICE) and Electrical Machine (EM) provide power to the wheels. The energy management is a key point of the operating of HEVs as it highly influences the fuel economy. In fact, it determines the propulsion mode (electric, hybrid or thermal) and the power sharing between the ICE and the EM.

On the other hand, the sizing of the electrical machine is probably one of the most common optimization problems in electromagnetic research [1] [2] [3]. Usually, the problem is to maximize the efficiency of the EM for given operating points subjected to external constraints such as weight, thermal, physical limitations, etc. In a dynamic system, where operating points of the EM are not *a priori* known, the problem is more complex.

In fact, in HEVs, the energy management highly influences the operating of the electrical machine. And, the size and performances of the machines highly interfere with the management. Moreover, the sizing of the other components (ICE, gear, etc.) has a high impact on the operating of the machine. The classical design process usually performed for HEVs consists in sizing energetically the system using coarse models of components such as efficiency maps for the EM [2] [4]. It fixes the constraints on the components (battery number of elements, engine and electrical machine minimum required torque, etc.) and the energy management

[3]. Then, the components are sized (using fine model) independently of their interaction with the system and of their effect on the management laws. It is clear that this method can easily lead to sub-optimal global solution.

Thus, in this context, the authors proposed to develop a global optimization. The proposed method will consider the control problem (energy management) as a sub-problem embedded in a global sizing optimization. In this work, the optimal control method using discrete dynamic programming DDP [5] [6] is chosen (section 2.B). The proposed design uses a fine, but fast enough to compute, electrical machine model (section 2.A). This design leads to the optimization of the electrical machine and other component characteristics (gear ratio, battery size, ICE power, etc.) in one global optimal design taking into account the influences between components, energy management and mission of the vehicle.

The first section of this paper details the modeling of the electrical machine and its validation with finite element method (FEM). The optimization process is then presented in a second section. This section also includes the presentation of the vehicle model. The third section presents the global sizing method proposed in the paper. A brief remaining on the optimal control problem which can be seen as a sub-optimization problem is also presented. The last section presents the results obtained with such a method for different driving conditions in terms of fuel economy and electrical machine geometries.

## **2. Modeling of the HEV**

### *2.A. Modeling of the electrical machine*

Usually, in HEV system's design, the Electrical machine (EM) is modelled using efficiency maps and applying scaling factor on torque, losses, power, etc. [4] [2][6]. Such approach leads to a lack of accuracy (efficiency and maximum torque) especially considering that in our application the power of the EM varies from 5 to 50 kW. Moreover, there is no degree of freedom on the "geometries" of the machine whereas it can highly change the efficiency area and thus the operating of the machine considering optimal management. Thus, in this work, authors proposed to use an EM model taking into account geometrical parameters (see section 3.A).

In this study, an internal permanent magnet synchronous motor is chosen as it is the most used machine in electrical power train. The EM is represented by a magnetic equivalent circuit model (i.e. a reluctance circuit) (MECM), using *Reluctool* software tool [7] [8] [9]. In such a model, flux tubes are represented by reluctances. For sizing, reluctance expressions depend on geometrical parameters, (e.g. air-gap length, magnet sizes, stator external radius...) and winding characteristics. A possible circuit model of one pole of the EM is presented in Fig. 2.

The MECM is fast to compute (around 100 ms), and takes into account non-linear phenomena, such as magnetic saturation. The magneto motive forces depend on the stator current and the magnetic reluctances depend on the geometrical parameters and the magnetic characteristics of materials. The resolution of this non-linear circuit is based on the Hopkinson's law and uses Newton-Raphson algorithm. This leads to the flux linkage  $\phi$  and the induction field ( $B$ ) in each magnetic reluctances.

To dispose of the static torque of the machine for different internal electrical angles, the rotation of the machine rotor is simulated by a multi-static solving. To avoid a change of MECM at each position, the rotor is considered to be fixed and the stator currents are changed to simulate the rotation. This is equivalent to a rotor

rotation with fixed stator currents. This allows fast solving of the MECM (which remains the same) and very lower model size (so need of RAM memory). The drawback of such a method is that the torque ripple cannot be considered. In fact, the reluctance scheme corresponds to those with magnetic pole aligned to stator teeth. Intermediary positions have to be taken into account to simulated torque ripples. For that, reluctance schemes with almost two times more reluctances parameterized by the rotor position are needed.

In the *Park's* reference (rotating bidirectional reference), the knowledge of the direct and the quadratic flux linkage  $\phi_d$  and  $\phi_q$  leads to the first harmonic of the direct and quadratic voltage  $v_d$  and  $v_q$ :

$$\begin{cases} v_d = R_s i_d - \omega \Phi_q \\ v_q = R_s i_q + \omega \Phi_d \end{cases} \quad (1)$$

where  $i_d$  and  $i_q$  are respectively, the direct and the quadratic current,  $\omega$  is the electrical pulsation of the electrical machine and  $R_s$  is the electrical resistance of one stator phase.

The calculation of the electrical power leads to the estimation of the mechanical mean torque  $\Gamma_{em}$ , for an active sign convention, i.e.  $\Gamma_{em}$  positive in the motor mode :

$$\Gamma_{em} = \frac{3}{2} p (\Phi_d i_q - \Phi_q i_d) - \frac{P_{iron} + P_f}{\Omega_{em}} \quad (2)$$

where  $P_{iron}$  and  $P_f$  are respectively, the iron losses and the mechanical losses.  $p$  is the number of pole pairs and  $\Omega_{em}$  is the rotation speed of the electrical machine. The iron losses are calculated thanks to a first harmonic Bertotti's model in each magnetic reluctance, taking into account hysteresis, excess and eddy-current losses [10] [11]. Mechanical losses are assumed to be proportional to the square of the external radius of the electrical machine and proportional to the rotation speed [12].

## 2.B. Validation of the electrical machine model

In order to estimate the validity of this model for a global sizing process, a model validation of the magnetic circuit model has been made using a finite element method (FEM) with Flux2D. The initial geometrical characteristics and manufacturing assessment come from pictures and measurements of the Toyota Prius 2004 EM [12]. This initial machine is simulated using a magneto static method. This model allows an accurate computation of flux linkage, torque and losses for different mechanical operating points. Fig. 3 presents a comparison between flux linkage computed with the MECM and the FEM models. The flux linkage is represented versus the internal electrical angle, i.e. the angle between the current and the q-axis in Park's reference. One can see the good agreement of the MECM with the fine model (FEM). The evaluation error is lower than 5% for all the internal electrical angle possible ranges. MECM presents a good accuracy to calculate flux linkages (Fig. 3). The torque is also in good accordance with those obtained with FEM method (Fig. 4) except for the torque ripple which is not simulated with our model (section 2.A). A MECM model appears then to be relevant for an optimal global sizing process. It is fast enough (100 ms) to be called thousands of times.

## 2.C. Modeling of the hybrid electrical vehicle

The vehicle model is based on a systemic approach. Schematic representation and notations are presented in Fig. 5.

The modeling of the HEV is based on the knowledge of the driving cycle (vehicle speed with respect to time). An upstream approach from wheel to components allows to calculate the ICE operating point in a backward manner. Knowing the vehicle weight and inertia, the vehicle acceleration leads to the required wheel torque  $\Gamma_w(t)$ . Knowing the demanded wheel torque and speed, and the gear box ratio, the torque and the speed before the first clutch are given by the following equations:

$$\Gamma^*(t) = \frac{\eta_{red}^{s(t)}}{k_{bv}(t)k_{red}} \Gamma_w(t) \quad (3)$$

$$\Omega^*(t) = \begin{cases} \text{If } u_2(t) = 0 \text{ or } (u_1(t) = 1 \text{ and } k_{bv}(t)k_{red}(t)\Omega_w(t) > \Omega_{ice}^{\min}) \\ \Omega^*(t) = k_{bv}(t)k_{red}(t)\Omega_w(t) \\ \text{else} \\ \Omega^*(t) = \Omega_{ice}^{\min} \end{cases} \quad (4)$$

where  $k_{bv}(t)$  is the gear box ratio at instant  $t$ ,  $k_{red}$  is the reduction gear ratio and  $\eta_{red}^{s(t)}$  is the efficiency of the final gear with respect to the power flow direction :  $s(t) = \text{sign}(\Gamma^* \Omega^*)$ .  $u_2(t)$  represents the state of Clutch 2 (closed if  $u_2(t)=1$  and open if  $u_2(t)=0$ ).

In hybrid propulsion mode (Clutch 2 closed),  $u_2(t)=1$  :

$$\Gamma_{ice}(t) = \Gamma^*(t) - \frac{\eta_{cpl}^{s(t)}}{k_{cpl}} (\Gamma_{em} i_{bat}(t) - J_{em} \frac{d\Omega_{em}}{dt}) + J_{em} \frac{d\Omega_{ICE}(t)}{dt} \quad (5)$$

$$\Omega_{ice}(t) = \Omega^*(t) \quad (6)$$

where,  $\Gamma_{ice}$  and  $\Omega_{ice}$  are respectively the engine torque and speed,  $\Gamma_{em}$ ,  $\Omega_{em}$ , and  $J_{em}$  are respectively the electrical machine torque, speed and inertia.  $\eta_{cpl}$  and  $k_{cpl}$  are the efficiency and ratio of the coupling device.

In electrical propulsion mode  $u_2(t)=0$  :

$$0 = \Gamma^*(t) - \frac{\eta_{cpl}^{s(t)}}{k_{cpl}} (\Gamma_{em} i_{bat}(t) - J_{em} \frac{d\Omega_{em}}{dt}) \quad (7)$$

$$\Omega_{mt}(t) = 0 \quad (8)$$

The model of the battery is a classical serial open circuit voltage source and resistance. The electromotive force  $E$ , depends on the state of charge,  $soc(t)$ . The serial resistance depends on the battery state of charge and current.

The ICE model is made using a specific fuel consumption (SFC) map (Fig. 6). The colored lined represents the specific fuel consumption, *i.e* the fuel burned in grams to produce one kW/h of mechanical energy on the shaft of the engine. Up and low torque limits are represented with a solid black line. The low bound correspond to the engine breaking with zero fuel consumption.

During the sizing process, the maximal power of the ICE,  $P_{ICE}$  is changed applying a scaling factor on the torque and the fuel consumption ( $\alpha_{ICE}=P_{ICE}/P_{ICE_{nom}}$ ). It is usually assumed that the power density is constant and lengths proportional to  $\alpha_{ICE}^{1/3}$  [2]. Mass moments of inertia have units of dimension  $M.L^2$ , this leads to a mass proportional to  $\alpha_{ICE}$  and a moment of inertia proportional to  $\alpha_{ICE}^{5/3}$ . The SFC remains thus the same.

### 3. Optimization of the sizing of the HEV

#### 3.A. Optimization problems

The optimization parameters taken into account in the paper are the number of NiMh modules ( $N_{bat}$ ), the continuous voltage of the converter ( $U_{bus}$ ) the ratios ( $k_{cpl}$ ,  $k_{red}$ ), the standard power of the ICE ( $P_{ICE}$ ), and geometrical parameters of the EM ( $X_{em}$ ). Fig. 7 presents the geometrical parameters of the EM.  $X$  is defined as the set of the 15 optimization variables. All of them are continuous.

$$X = \{N_{bat}, U_{dc}, P_{ice}, k_{cpl}, k_{red}, X_{em}\} \quad (9)$$

$$X_{em} = \{RHQ, RAD1, LM, GAP, \alpha, H3S, H4S, W3S, MAGWID, Depth\}$$

The objectives to minimize are the fuel consumption over a driving cycle ( $J_1$ ) and the number of battery modules ( $N_{bat}$ ):

$$J_1 = \int_{t_0}^{t_f} \dot{m}_{fuel}(i_{bat}(t), u_2(t), X) dt \quad (10)$$

where  $\dot{m}_{fuel}$  is the instantaneous fuel rate,  $u_2(t)$  the state of clutch 2,  $i_{bat}$  the battery current and  $X$  the optimization parameter set (9).

The main constraints to be respected are:

- geometrical constraints on the electrical machine
- battery state of charge (soc) at the end of the driving cycle (section 3.B)
- dynamic performances of the vehicles, determined using the previously presented vehicle model; Table 1 presents the constraints used below.

Fig. 8 shows the optimization strategy of the sizing of the parallel-HEV. The control problem is considered as a sub-optimization problem embedded in the global optimization of the sizing of the vehicle. The global sizing optimization is performed using multi-objective NSGA-II algorithm [13]. This allows to perform a multi-objective optimization and to dispose of a Pareto front which allows to choose an architecture after the optimization process. The optimization has been carried out using NSGA-II implementation from Matlab.

Consequently, this problem involves 15 optimization variables and 10 constraints. The computation time of the objective for one set of parameters and a driving cycle of 556s (1s step time), is about 16s with an i7-2630 QM processor and 8Go RAM. The global optimization time, with 60 individuals and 500 generations is about 24h using a 6 cores parallel computation.

As said before, in the paper, the two objectives to be minimized are: the fuel consumption and the battery number. Nevertheless, with this approach, it becomes easy to add objectives representing the cost or the volume of raw material for example. In future works, this will be really useful to make a choice after sizing process regarding economic criteria.

### *3.B. Optimal control problem*

The control problem is a key point of HEV operating and is even more critical in global design process.

For real time implementation in vehicle, a rule-based strategy is usually used. However, such a strategy highly depends on the sizing of the vehicle and on the efficiency of the components. Thus, it can be relevant for one sizing and not for another. To avoid this non monotonic effect in an optimization process, the authors chose to use the optimal energy management (OEM), based on optimization methods. This leads to the optimal fuel consumption of the vehicle for a given set of parameters and thus allows a fair comparison between different sizings. However, this strategy requires the knowledge of the driving cycle in advance.

In the proposed method, the discrete dynamic programming (DDP) [5] [6] [14] is used and is solved at each step of the sizing optimization. A good representation of this optimization problem is a SOC versus time graph (Fig. 9) limited by maximum battery charge and discharge capabilities. The constraint on the final SOC is obviously respected by the building of the limits (Fig. 9).

This graph is regularly sampled in time and SOC. The points of two consecutive columns are linked by oriented edges associated to a fuel consumption. This fuel consumption depends on the drive cycle profile and the SOC variation between the two points of an edge. It is calculated using the previously presented vehicle model (section 2.C). The sum of fuel consumption of the edges on a trajectory provides the objectives to minimize. The DDP method is then applied to find the best trajectory in an efficient way [5] [6].

## **4. Results**

This section presents the results obtained when using the previously proposed method. Different driving cycles representing urban road and highway conditions are used. A first initial sizing is described to provide a reference.

### *4.A. Initial sizing and performances of the hybrid electrical vehicle*

The initial sizing (Table 2) is based on those of the Toyota Prius II. The number of battery elements is 28 leading to a global battery power of 30 kW. The initial geometry of the machine corresponds to those of the Prius and has a power of 50kW.

In our case of parallel architecture, the EM machine power is normally chosen equal to the standard power of the battery pack. The EM has thus been downsized using a scaling factor on every dimension (see section 3.A).

The coupling ratio is chosen to be 0.7 so that the optimal rotation speed of the electrical machine matches with the optimal rotation speed of the internal combustion engine. Gear box ratios, ICE and reduction

ratio are based on an existing conventional vehicle, which is the Renault Clio. The initial ICE fuel consumption map is presented Fig. 6.

Initial fuel consumptions of the vehicle are shown in Table 3.

#### *4.B. Result for several driving conditions*

The global optimization process has been applied to three different driving cycles. About 27000 simulations are needed for each cycle. Computation time depends on the driving cycle length and varies from 16h to 24h. This optimization is performed using parallel computing (8 cores).

Fig. 10 presents the Pareto front –number of battery elements versus fuel consumption- obtained for urban driving conditions. All the simulated individuals are plotted. The corresponding Pareto front is represented in bold.

One can see that there is a compromise between the battery pack size and the fuel consumption over the driving cycle. The fuel consumption logically decreases when the number of battery elements increase. In fact, the battery can be used in a more efficient manner and in particular regenerative braking energy can be completely recovered. However, over a certain number of battery elements, no improvement can be obtained. The battery becomes more and more heavy and cannot be used in a more efficient manner.

Table 3 presents the optimal design obtained for 25 elements in the battery pack which seems a good trade off -fuel consumption versus battery numbers- in the Pareto front. It is compared to the initial sizing of the electrical machine and the component. Fig. 11 presents the corresponding obtained geometries of the electrical machine.

In Table 3, it clearly appears that the fuel consumption is reduced from 10% with the proposed optimal method compared to an initial design based on existing components. Going from urban driving conditions to highway conditions the power of the EM decreases when those of the ICE increases. This can be explained by considering that pure electrical modes (propulsion and regenerative braking) are more involved and efficient in urban conditions, whereas ICE is highly involved in highway condition.

Fig. 11 shows that, compared to the initial geometry, the volumes of magnet and copper increase. This probably allows improving the efficiency of the EM on its operating point; this, taking in mind that global optimization leads to the best trade-off between EM and ICE efficiency.

Efficiency maps of initial sizing and the optimal solution for the urban cycle and operating points over the urban driving cycle are presented in Fig. 12. First, we note that both EM are over-sized considering the operating points. This is due to a compromise between the standard powers of the ICE because the total installed power is mainly constrained to the dynamical performances. One can see the differences on the torque limits. It is mainly explained by the copper section difference and the maximal voltage available (c.f. Table 3). Comparing both simulations, we can measure an improvement of 3.34% of the EM efficiency over the whole cycle. Over the urban driving cycle, the fuel consumption gain between the two sizings can be partly explained by a better use of the EM.



## 5. Conclusion

This paper proposes a new global optimization method to size the power train of a hybrid vehicle. The EM is sized at the same time as its surrounding components (gear, battery ...). For that, a fast but accurate model of the EM using magnetic circuit model has been developed. The energy management control problems, which highly interfere with the components size and efficiency is solved using DDP optimal method. This allows a fair comparison between the different sizings and avoids the non-monotonic effect of energy management in the sizing process.

DDP is embedded in a multi-objective genetic optimization with EM geometrical parameters and system parameters. This provides the Pareto front fuel consumption/battery number of elements. The time calculation (16 to 24h) proves the feasibility of such an approach (optimal control and fine EM model embedded in NSGA algorithm). The results shows an improvement on fuel consumption around 10% compared to an initial sizing based on decoupled approach.

Pareto front including economical consideration can easily be obtained adding a cost or volume of raw material objectives. This allows an *a posteriori* choice of the final architecture of the drive train considering the actual price of material and fuel.

This method is currently applied to more complex hybrid architectures containing two or more electrical machines.

## 6. Acknowledgments

Funding for this project was provided by a grant from *la Région Rhône-Alpes*.

## 7. References

- [1] P. Di Barba, M. Bonislawski, R. Palka, P. Paplicki and M. Wardach, "Design of Hybrid Excited Synchronous Machine for Electrical Vehicles," *IEEE Transaction on Magnetics*, vol. 51, no. 8, 2015.
- [2] C. Bertram, D. Buecherl, A. Thanheiser and H. Herzog, "Multi-objective optimization of a parallel hybrid electric drive train," in *Vehicle Power and Propulsion Conference (VPPC)*, 2011.
- [3] K. Chau, C. Chan and C. Liu, "Overview of permanent-magnet brushless drives for electric and hybrid electric vehicles," *Industrial Electronics, IEEE Transactions on*, vol. 55, no. 6, p. 2246–2257, 2008.
- [4] S. Buerger, B. Lohmann, M. Merz, B. Vogel-Heuser and M. Hallmannsegger, "Multi-objective optimization of hybrid electric vehicles considering fuel consumption and dynamic performance," in *Vehicle Power and Propulsion Conference (VPPC), 2010 IEEE*, 2010.
- [5] R. Bellman, "Dynamic programming and Lagrange multipliers," *Proceedings of the National Academy of Sciences of the United States of America*, vol. 42, no. 10, p. 767, 1956.

- [6] D. E. Kirk, *Optimal control theory: an introduction*, Courier Dover Publications, 2012.
- [7] B. Du Peloux, L. Gerbaud, F. Wurtz, V. Leconte and F. Dorschner, "Automatic generation of sizing static models based on reluctance networks for the optimization of electromagnetic devices," *Magnetics, IEEE Transactions on*, vol. 42, no. 4, pp. 715-718, 2006.
- [8] X. Nguyen, L. Gerbaud, L. Garrbuio and F. Wurtz, "Computation Code of Software Component for the Design by Optimization of Electromagnetical Devices," *Magnetics, IEEE Transactions on*, vol. 50, no. 2, 2014.
- [9] B. Delinchant, D. Duret, L. Estrabaut, L. Gerbaud, H. N. Huu, B. Du Peloux, H. L. Rakotoarison, F. Verdi{\`e}re and F. Wurtz, "An optimizer using the software component paradigm for the optimization of engineering systems," *COMPEL: The International Journal for Computation and Mathematics in Electrical and Electronic Engineering*, vol. 26, no. 2, pp. 368-379, 2007.
- [10] G. Bertotti, "General properties of power losses in soft ferromagnetic materials," *Magnetics, IEEE Transactions on*, vol. 24, no. 1, p. 621-630, 1988.
- [11] F. Magnussen, Y.-K. Chin, J. Soulard, A. Broddefalk, S. Eriksson and C. Sadarangani, "Iron losses in salient permanent magnet machines at field-weakening operation," in *Industry Applications Conference, 39<sup>th</sup> IAS Annual Meeting*, 2004.
- [12] J. Hsu, C. Ayers, C. Coomer, R. Wiles, S. Campbell, K. Lowe and R. Michelhaugh, Report on Toyota/Prius Motor Torque-Capability, Torque-Property, No-Load Back EMF, and Mechanical Losses, United States. Department of Energy, 2004.
- [13] K. Deb and others, *Multi-objective optimization using evolutionary algorithms*, vol. 2012, John Wiley&Sons Chichester, 2001.
- [14] E. Vinot, R. Trigui, B. Jeanneret, J. Scordia and F. Badin, "HEVs comparison and components sizing using dynamic programming," in *Vehicle Power and Propulsion Conference*, 2007.
- [15] Flux2D, *Flux 2D*, available at <http://www.cedrat.com/en/software/flux.html>.
- [16] V. Reinbold, E. Vinot and L. Gerbaud, "Global optimization of a parallel hybrid vehicle using optimal energy management," *International Journal of Applied Electromagnetics and Mechanics*, vol. 43, no. 1, pp. 115-126, 2013.

Table 1. Dynamic performances constraints

Acceleration time from 0 to 100 km/h (s)	Maximal vehicle speed (km/h)	Time to overpass a truck driving at 80 km/h (s)
$t_{0 \rightarrow 100}$	$V_{\max}$	$T_{\text{pas}}$
12.0	160	9.0

Table 2. Initial hybrid vehicle sizing

<i>Standard power of the EM</i>	30	kW
<i>Base speed of the EM</i>	1420	tr.min <sup>-1</sup>
<i>Maximal torque of the EM</i>	200	N.m <sup>-1</sup>
<i>Continuous voltage : <math>U_{bus}</math></i>	330	V
<i>Internal combustion power: <math>P_{mt}</math></i>	50.6	kW
<i>NiMh module number : <math>N_{bat}</math></i>	28	
<i>Battery pack standard power</i>	29.5	kW
<i>Coupling ration : <math>k_{cpt}</math></i>	0.7	
<i>Reduction gear ratio: <math>k_{red}</math></i>	3.2941	

Table 3 Optimal design obtained for 25 battery number of elements

Optimized parameters							Raw material volume (m <sup>3</sup> )		Fuel consumption (l/100km)		
sizing	N <sub>bat</sub>	U <sub>bus</sub> (V)	P <sub>em</sub> (kW)	P <sub>ice</sub> (kW)	k <sub>cpl</sub>	k <sub>red</sub>	copper volume	copper magnet	urban	road	highway
initial	28	330	30	54.4	0.7	3.294	0.9607	0.774	2.77	3.04	4.36
urban	25	221	29.9	31.9	0.596	2.658	1.874	1.442	2.51		
road	25	205	27.1	33.2	0.566	2.65	2.056	1.374		2.78	
highway	25	209	24.3	39.3	0.475	2.408	1.846	1.134			3.98

Fig. 1 Parallel HEV architecture

Fig. 2 MECM circuit of the electrical machine using Reluctool

Fig. 3 Validation of the flux linkage computing with finite element method (FE) and  $I_{me} = 200$  A

Fig. 4 Validation of the torque with finite element method

Fig. 5 Modeling of the hybrid drive train

Fig. 6 Specific fuel consumption (g/kW.h) map of ICE

Fig. 7 Geometrical parameters of the EM

Fig. 8 Optimization strategy

Fig. 9 DDP principle

Fig. 10 Pareto front battery versus fuel consumption for urban driving cycle

Fig. 11 (a) Initial EM geometry, (b) urban driving cycle, (c) road driving cycle, (d) highway driving cycle

Fig. 12 Comparison of operation points and efficiency map between the initial sizing and the urban optimal solution

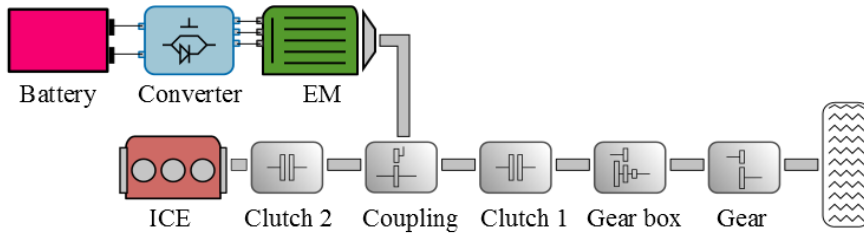


Fig. 1 Parallel HEV architecture

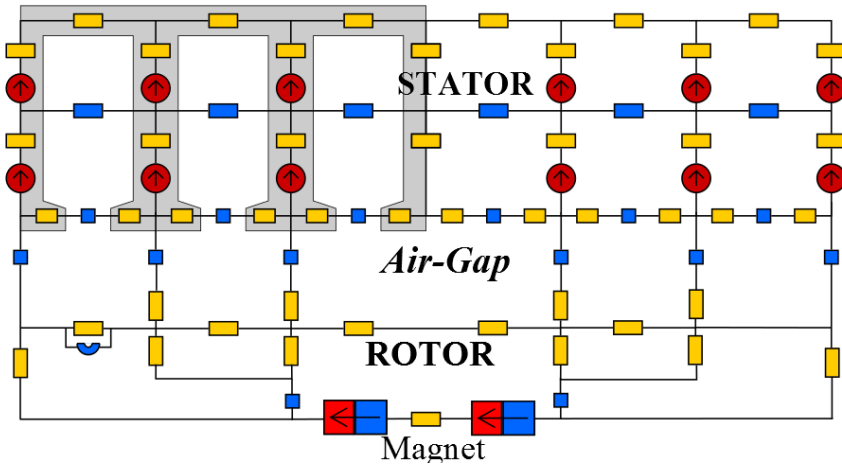


Fig. 2 MECM circuit of the electrical machine using Reluctool



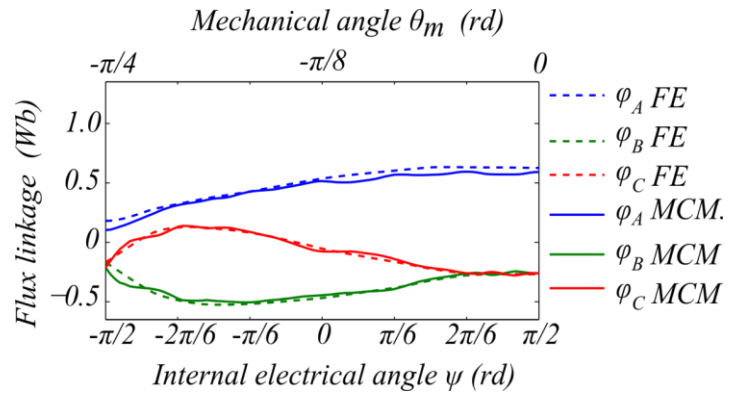


Fig. 3 Validation of the flux linkage computing with finite element method (FE) and  $I_{me} = 200$  A

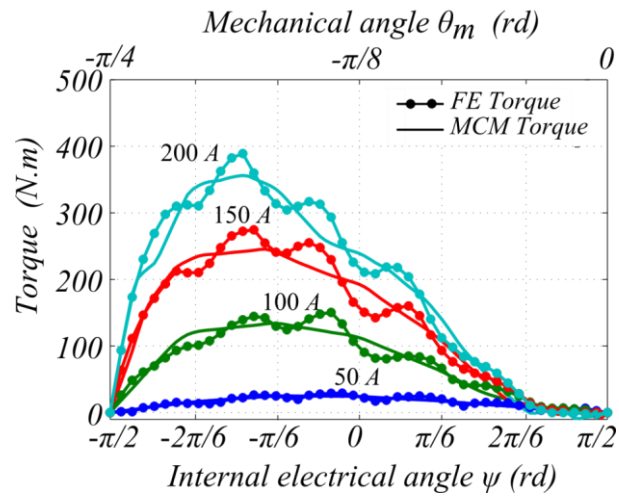


Fig. 4 Validation of the torque with finite element method

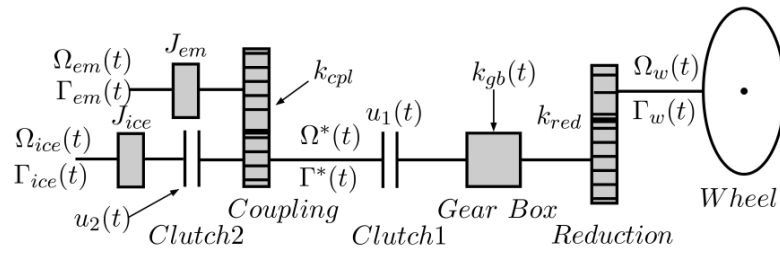


Fig. 5 Modeling of the hybrid drive train

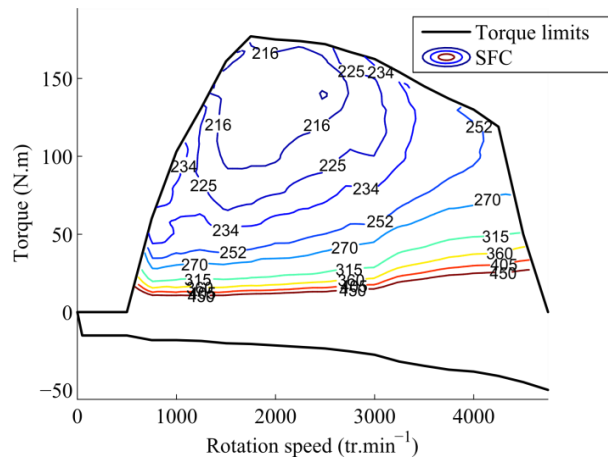


Fig. 13 Specific fuel consumption (g/kW.h) map of ICE

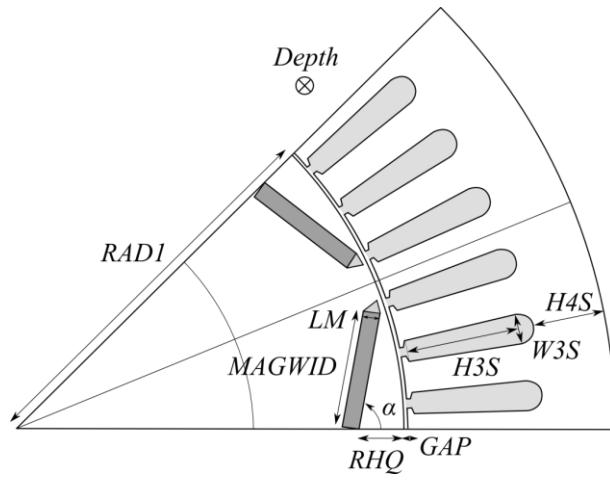


Fig. 7 Geometrical parameters of the EM

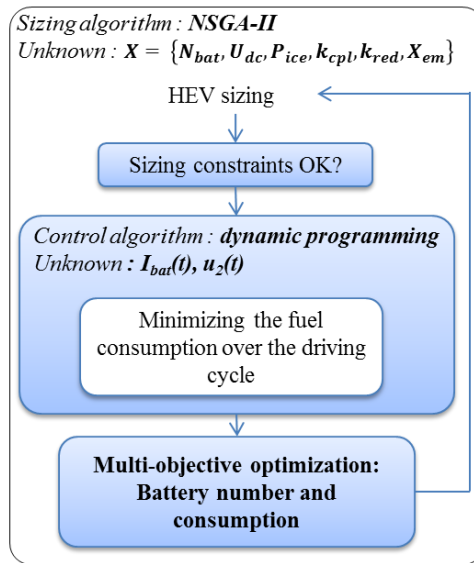


Fig. 8 Optimization strategy

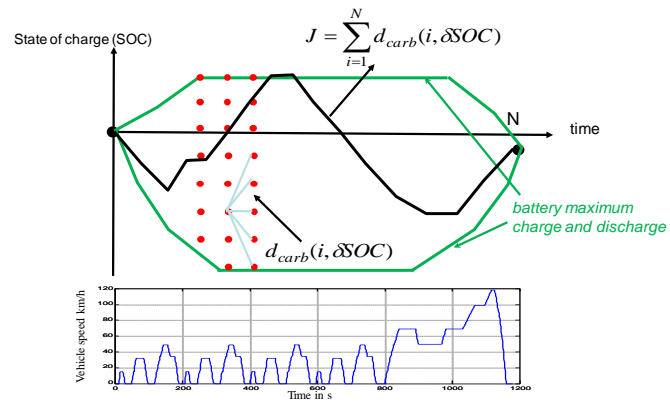


Fig.9 DDP principle

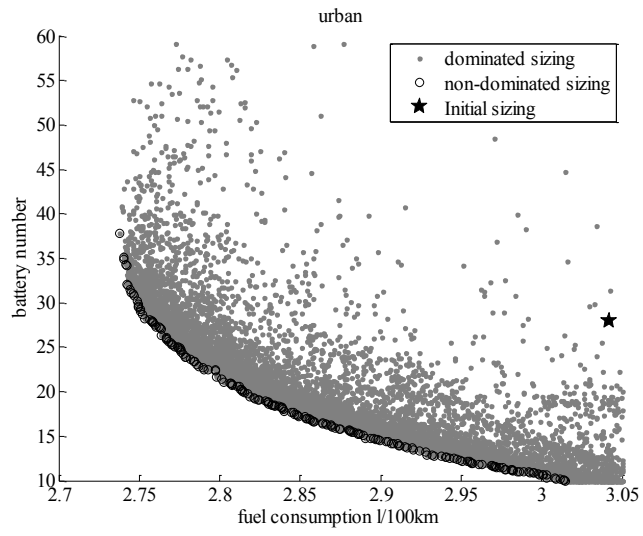


Fig. 10 Pareto front battery versus fuel consumption for urban driving cycle



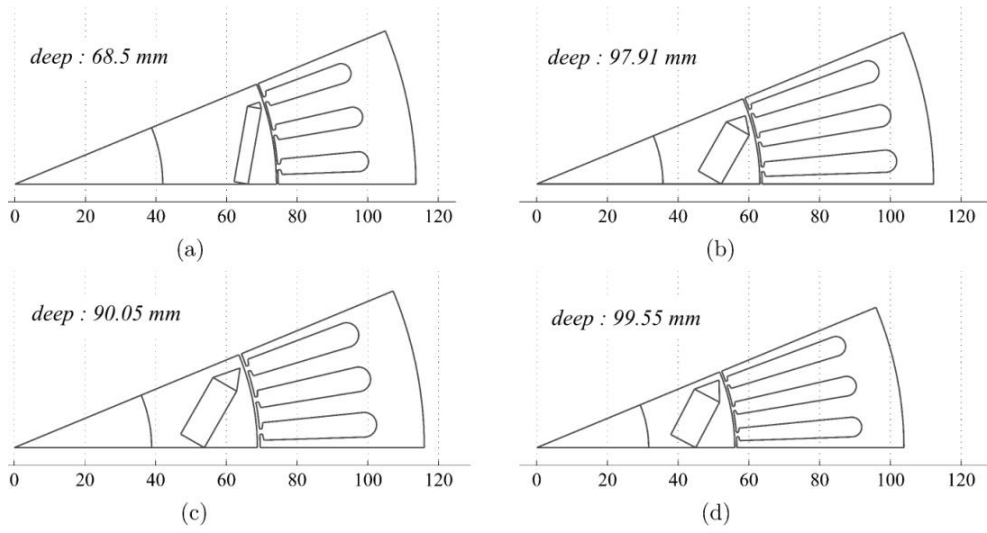
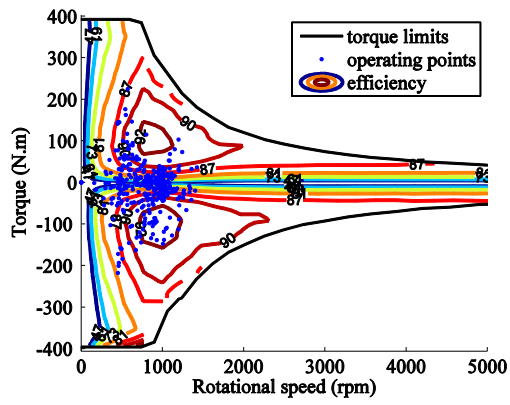
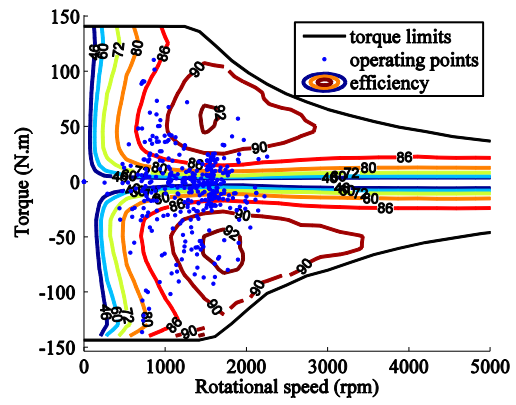


Fig. 11 (a) Initial EM geometry, (b) urban driving cycle, (c) road driving cycle, (d) highway driving cycle



(a) initial EM geometry



(b) urban driving cycle

Fig. 12 Comparison of operation points and efficiency map between the initial sizing and the urban optimal solution